Proceedings of ISERME 2025
19-20 September 2025
https://doi.org/10.31705/ISERME.2025.20

Property Enhancement of Graphite-Based-Battery

Sampath LPSS, Ranasinghe EH, Kirushan P, *Rohitha LPS, Rathnayake NP, Abeysinghe AMKB, Premasiri HMR, AVP, Wickramarachchi WASM

Department of Earth Resources Engineering, University of Moratuwa, Sri Lanka

*Corresponding author – rohitha@uom.lk

Abstract

This study presents a comparative evaluation of graphite oxide (GO) and microwave-exfoliated graphite oxide (MEGO) as anode materials for sodium-ion batteries, with synthesized sodium manganese oxide ($NaMnO_2$) serving as the cathode. GO was prepared via a modified Hummers method, and MEGO was obtained by subjecting GO to microwave irradiation. Structural and morphological characterization was performed using X-ray diffraction (XRD), scanning electron microscopy (SEM), and quantitative image analysis with ImageJ software. Morphological analysis revealed that GO exhibited enhanced surface area enhancement (88.8% increase) compared to raw graphite. Surface roughness analysis demonstrated progressive texture enhancement, with microwave treatment contributing 75% of total surface roughness improvement. Sodium manganese oxide ($NaMnO_2$) cathodes were synthesized using both analytical-grade and recovered MnO_2 from spent Zn-MnO_2 batteries. XRD analysis revealed that recovered MnO_2 unexpectedly demonstrated enhanced phase purity (83% identified phases) compared to analytical-grade material (43% identified phases). Electrochemical testing showed GO-based anodes delivered approximately twice the capacity (0.232 mAh) compared to MEGO anodes (0.107 mAh), with better voltage stability and discharge duration. The results demonstrate the feasibility of utilizing recycled battery materials for cathode synthesis while establishing GO as a more promising anode material than MEGO for sodium-ion battery applications.

Keywords: Battery recycling, Electrochemical performance, Graphite oxide, Manganese dioxide, Microwave exfoliation, Sodium-ion batteries

1 Introduction

The increasing global demand for efficient and sustainable energy storage solutions has driven significant advancements in battery technologies. Among these, graphite-based systems have gained attention as promising candidates due to their low cost, natural abundance, and favourable electrochemical properties. In Sri Lanka, the availability of high-purity vein graphite presents a unique opportunity to develop cost-effective, locally sourced battery technologies. However, the practical implementation of advanced battery chemistries in such regions is often constrained by limited access to sophisticated processing equipment and high-end materials [1].

This study addresses these challenges by focusing on the enhancement of graphite-based batteries through the optimization of structural and material characteristics using methods that are both scientifically robust and regionally adaptable. Central to this research is the modification of raw graphite via the synthesis of graphite oxide (GO), followed by further structural enhancement through microwave treatment [2]. This dual-step modification strategy is designed to increase interlayer spacing and improve electrochemical activity [3], thereby overcoming the inherent limitations of graphite for sodium-ion intercalation in sodium-ion battery (SIB) systems. Despite its potential, the application of microwave-exfoliated GO in SIBs remains relatively underexplored [2].

In addition to anode modification, this study also investigates the extraction of MnO_2 from spent Zn–Mn batteries and the laboratory synthesis of sodium manganese oxide ($NaMnO_2$) as the cathode material. The cathode is prepared via a solid-state reaction using sodium carbonate (Na_2CO_3) and MnO_2 [4],[5] recovered from spent Zn–MnO_2 batteries, as well as analytical-

grade MnO_2. Furthermore, an ethanol-based sodium perchlorate ($NaClO_4$) [5] is employed as a more economical electrolyte. Collectively, these efforts aim to enhance battery performance and support the development of scalable, sustainable, and locally viable graphite-based energy storage solutions.

2 Experimental

2.1 Preparation of Graphite Oxide (GO)

Graphite oxide (GO) was synthesized using a modified Hummers method[6] starting with 1 g of graphite powder (<63 µm). The process began by mixing the graphite with 0.5 g $NaNO_3$ and 23 ml concentrated H_2SO_4 in a 500 ml flask at 5 °C for 5 minutes. Then, 3g of $KMnO_4$ was gradually added and the mixture was stirred at 5 °C for 2 hours, followed by heating to 35 °C for 30 minutes. The addition of 46 ml deionized water caused an exothermic reaction raising the temperature to 98 °C, where it was maintained for 30 minutes. The reaction was terminated by adding 140 ml deionized water and 10 ml hydrogen peroxide solution (10% v/v), producing a brown/yellowish suspension indicating GO formation. The product was filtered and washed five times with 200 ml diluted HCl solution (5%) to remove manganese ions, then washed with warm deionized water at 70 °C until neutral pH. Finally, the GO was dried at 60 °C for 12 hours to obtain the final powder.

2.2 Preparation of Microwave Exfoliated Graphite Oxide (MEGO)

The prepared graphite oxide (GO) powders were converted to microwave-exfoliated graphite oxide (MEGO)[2] using a GE microwave oven (Model JES0736SM1SS) at 700 W under ambient conditions. Four different exposure times were tested: 15 seconds, 30 seconds, 45 seconds, and 1 minute. During microwave treatment, the GO powders underwent significant volume expansion with vapor release and 'violent fuming'. The GO powder in a Teflon crucible expanded dramatically to form a black, fluffy powder characteristic of MEGO, as shown in Figure 1. The process required careful control as excessive microwave treatment of MEGO caused sparking and potential ignition, indicating that overexposure should be avoided to prevent combustion of the exfoliated material.

2.3 MnO2 Preparation from Spent Zn-Mn Batteries

In this work, used Zn–MnO_2 batteries of AA type were utilized as the source material. The pretreatment process involved manually disassembling the spent batteries and separating them into cathode materials and other components. The cathode material was thoroughly washed with deionized water to remove soluble salts and subsequently dried at 110 °C to a constant weight prior to weighing.

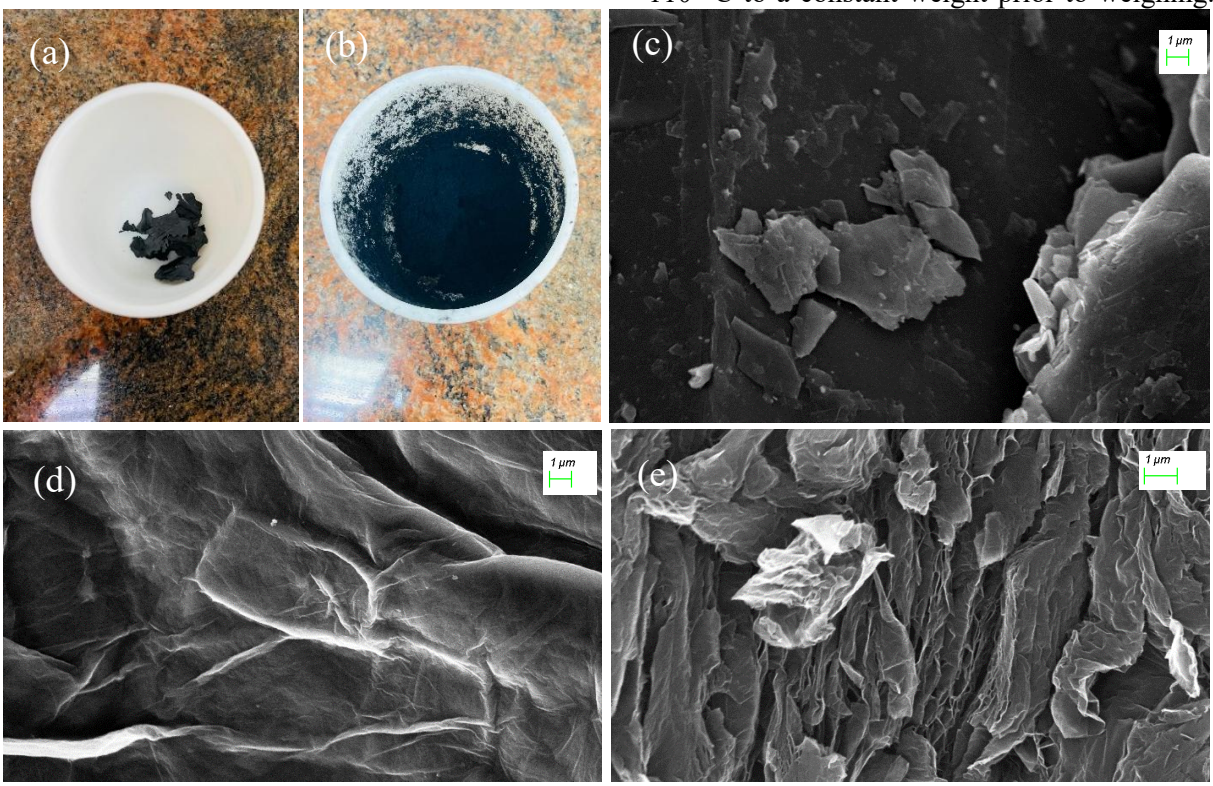

Figure 1: Optical photos of GO before (a) and after (b) treatment in a microwave oven for 1min. SEM image of raw graphite (c), GO (d), MEGO (e).

For the dissolution process, the cathode materials were treated with 0.50 M sulfuric acid (H_2SO_4) and 30% (v/v) hydrogen peroxide (H_2O_2) solutions. The optimized conditions established for the dissolution were 1.5 g of cathode material per 100.0 ml of 0.50 M H_2SO_4 and 1.0 ml of 30% (v/v) H_2O_2 solution. The addition of hydrogen peroxide served to prevent the oxidation of Mn^{2+} ions by dissolved oxygen present in the solution during the dissolution process. The cathode dissolution was carried out under constant magnetic stirring at a speed of 800 rpm and maintained at 35 °C for 3 hours. Following the dissolution of manganese oxides, the resulting suspension was filtered to separate the solid residues. The graphite component was recovered after filtration and further dried at 110°C for 12 hours[7].

$$MnO_{2(s)} + H_2SO_{4(aq)} + H_2O_{2(aq)} \rightarrow MnSO_{4(aq)} + 2H_2O_{(l)} + O_{2(g)} \quad (1)$$

To precipitate the ionic manganese, an aliquot of the dissolution solution was diluted to one-tenth of its original concentration. A 1.00 M ammonium hydroxide (NH_4OH) solution was then added as the precipitating agent to facilitate the formation of manganese hydroxide.

$$MnSO_{4(aq)} + 2NH_4OH_{(aq)} \rightarrow Mn(OH)_{2(s)} + (NH_4)_2SO_{4(aq)} \quad (2)$$

The resulting precipitation was separated from the supernatant by filtration. Subsequently, the collected precipitate was dried at 110 °C for 12 hours, during which the mass of the manganese oxide remained constant, indicating complete.

2.4 Preparation of Sodium Manganese Oxide ($NaMnO_2$)

Sodium manganese oxide ($NaMnO_2$) was synthesized via a solid-state reaction method. Two precursor sources for MnO_2 were employed: MnO_2 recovered from spent Zn–MnO_2 batteries and analytical-grade MnO_2 obtained from laboratory supplies, to compare the effects of precursor source on the final product properties. The Process Starting with thermal decomposition of MnO_2 at 600°C for 4 hours to produce Mn_2O_3. The Na_2CO_3 was crushed using a trimmer mill and sieved through 63-micron mesh to ensure uniform particle size. The Mn_2O_3 and Na_2CO_3 were mixed in stoichiometric ratios and subjected to ball milling for homogeneous powder formation. Ethanol was added as a binding medium to facilitate pellet formation, and the mixture was shaped into uniform pellets using a pellet press. After ethanol evaporation, the dried pellets were calcined at 850°C for 10 hours[5], then slowly cooled and stored in a desiccator to prevent atmospheric contact, completing the $NaMnO_2$ synthesis.

$$4MnO_2 \xrightarrow[600\,^\circ C]{4h} 2Mn_2O_3 + O_2 \quad (3)$$

$$Na_2CO_3 + Mn_2O_3 \xrightarrow[850\,^\circ C]{10h} 2NaMnO_2 + O_2 \quad (4)$$

2.5 Electrochemical Cell

The anode was prepared by applying a 0.5 mm thick layer of synthesized expanded graphite, mixed with deionized water and Araldite as a binder, onto a 4 cm² area of Cu foil, followed by

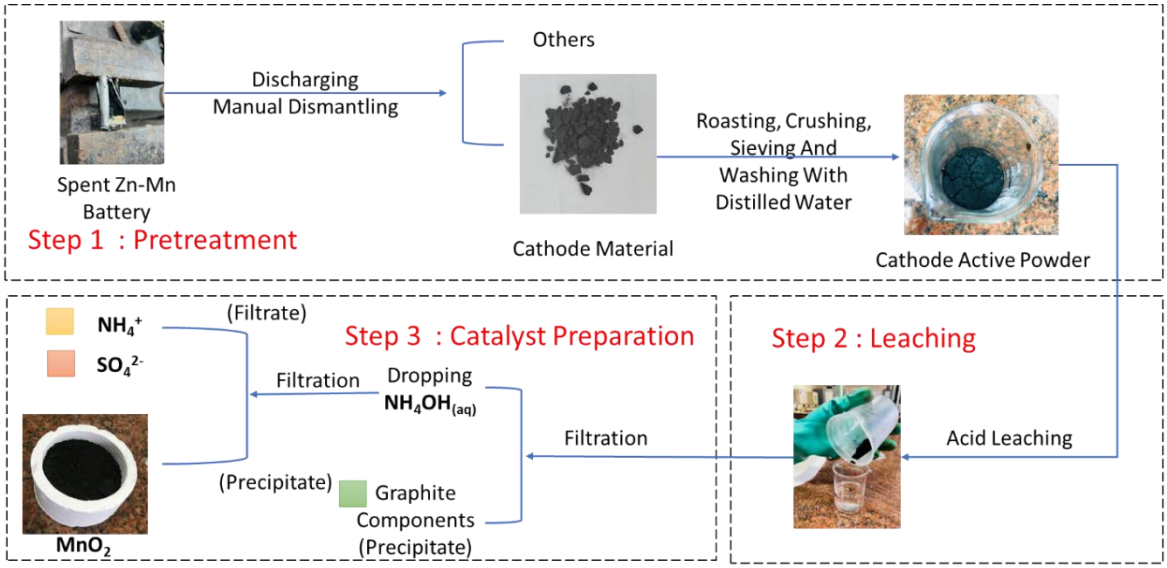

Figure 2: Process of MnO2 Preparation from Spent Zn-MnO2 Batteries.

drying at 80 °C for 20 minutes. Similarly, the cathode was fabricated using Al foil coated with synthesized $NaMnO_2$, using acetone and Araldite as binders.

The electrolyte was synthesized by reacting magnesium perchlorate with sodium carbonate in water, filtering out the $MgCO_3$ precipitate, drying the resulting $NaClO_4$ at 110 °C, and dissolving it in ethanol.

Separators were prepared by cleaning used separating papers through sequential treatments with ethanol, diluted nitric acid, and hydrogen peroxide to remove contaminants, ensuring suitability for sodium-ion cell assembly.

2.6 Characterization Techniques

The sample structure was characterized using X-ray diffraction (XRD) with a Cu K-α radiation source (λ = 1.5405 Å) and a K-beta filter. Diffraction data were collected in the 2θ range of 5–80° at a scan rate of 2°/min. XRD data were processed using PDXL-2 software, and phase identification was performed using the International Centre for Diffraction Data (ICDD) database.

Scanning electron microscopy (SEM) was employed to examine the morphologies and surface characteristics of raw graphite, graphite oxide (GO), and microwave-treated graphite oxide samples using an acceleration voltage of

10.00 kV, working distance of 12.5 mm, and magnification range of 1.00 KX to 25.00 KX. Surface roughness and topography analysis were performed using ImageJ software with the Roughness/Waviness plugin to extract quantitative surface parameters including average roughness (Ra), maximum height (Rz), and mean spacing (RSm).

2.7 Electrochemical analysis

The voltage profile of the battery was monitored during charge–discharge cycles to assess voltage stability and consistency over time, providing insight into its ability to deliver a steady voltage during operation. Battery capacity was evaluated by monitoring the discharge process, recording the discharge current as a function of time until a predefined cutoff voltage was reached, and calculating capacity by integrating current over time.

3 Results and Discussion

3.1 Graphite Modification for Enhanced Anode Properties

3.1.1 Morphological Evolution and Structural Changes

The ImageJ software analysis revealed dramatic structural changes during graphite oxidation. Raw graphite contained 547 particles with a total surface area of 1,196,880 μm² and average particle size of 2,188 μm². After oxidation using the modified Hummer's method, the particle count decreased by 52.7% to 259 particles, indicating particle agglomeration. Despite this consolidation, the total surface area increased remarkably by 88.8% to 2,259,440 μm², demonstrating successful surface enhancement. The average particle size expanded dramatically by 298.6% to 8,723 μm², suggesting significant layer expansion and intercalation of oxygen-containing functional groups between graphene layers.

Table 1: Morphological parameters of raw graphite and graphite oxide samples showing surface area enhancement and particle size evolution during oxidation process.

Graphite Source	Particle Count	Total Area (μm²)	Average Size (μm²)	%Area	Mean	Perim.	Circ.	Solidity	Feret	MinFeret
Raw Graphite	547	1196880	2188	61.684	255	157.642	0.251	0.854	64.868	6.675
GO	259	2259440	8723	78.499	255	412.959	0.221	0.836	150.531	14.249

This morphological evolution confirms that oxidation effectively introduced functional groups and expanded interlayer spacing [3], creating a more accessible surface structure for subsequent modifications. Microwave-Induced Interlayer Expansion and Exfoliation: The microwave treatment analysis shows progressive interlayer expansion in graphite oxide with increasing exposure time. Mean expansion length increased from 205.111 nm (15 seconds) to 578 nm (60 seconds), representing a nearly three-fold enhancement. The intermediate values at 30 seconds (473 nm) and 45 seconds (556 nm) demonstrate consistent time-dependent expansion.

Table 2: The effect of microwave exposure on the interlayer spacing of graphite oxide (GO).

Time exposure for Microwave	Mean interlayer expansion length (nm)	Standard Deviation (nm)
15 sec	205	63
30 sec	473	249
45 sec	556	164
60 sec	578	185

The standard deviation values (63 to 249 nm) indicate some variability within samples due to heterogeneous exfoliation and localized differences in gas evolution. These results confirm that microwave treatment effectively promotes GO layer separation through rapid thermal effects and volatile release during irradiation.

3.1.2 Surface Roughness and Topography Analysis

Surface roughness analysis using ImageJ software with the Roughness/Waviness plugin revealed systematic enhancement of surface texture parameters throughout the graphite modification process (Table 3). The quantitative assessment of three key roughness parameters average roughness (Ra), maximum height (Rz), and mean spacing (RSm) demonstrates the progressive evolution of surface characteristics from raw graphite to the final microwave-treated material.

Table 3: Surface roughness parameters roughness (Ra), maximum height (Rz), and mean spacing (RSm) of raw graphite, graphite oxide, and 1-min microwave-treated GO samples.

Parameter	Raw Graphite	Graphite Oxide	1-min Microwave	Change (Raw→MW)	% Change
Ra (µm)	17	19	25	+7.83	+0.452
Rz (µm)	196	223	225	+28.93	+0.148
RSm (µm)	11	12	11	-0.54	-0.048

The surface roughness analysis shows that microwave treatment was the dominant factor in surface modification. Ra values increased from 17 units (raw graphite) to 25 units (final product), with microwave treatment contributing 75% of the total 47% enhancement compared to only 25% from oxidation.

The maximum height (Rz) parameter increased significantly during oxidation (196 to 223 units, +13.8%) but remained nearly unchanged during microwave treatment (225 units, +0.9%).

3.2 $NaMnO_2$ Cathode Material Synthesis and Characterization

3.2.1 XRD Phase Identification and Comparison of Solid-State Synthesis Using Different MnO_2 Precursors

X-ray diffraction analysis was performed to evaluate the crystalline structure and phase purity of $NaMnO_2$ synthesized using two different MnO_2 precursor sources. Figure 2 presents the XRD patterns of $NaMnO_2$ synthesized via solid-state reaction using sodium carbonate (Na_2CO_3) with (A) MnO_2 recovered from spent Zn–MnO_2 batteries and (B) analytical-grade MnO_2.

Phase identification was conducted using ICDD (PDF-2 Release 2015 RDB) reference databases. For the recovered MnO_2 sample, cards 01-072-0830 and 00-027-0752 were used, while the analytical-grade sample was analyzed using cards 01-072-0831 and 01-072-0830.

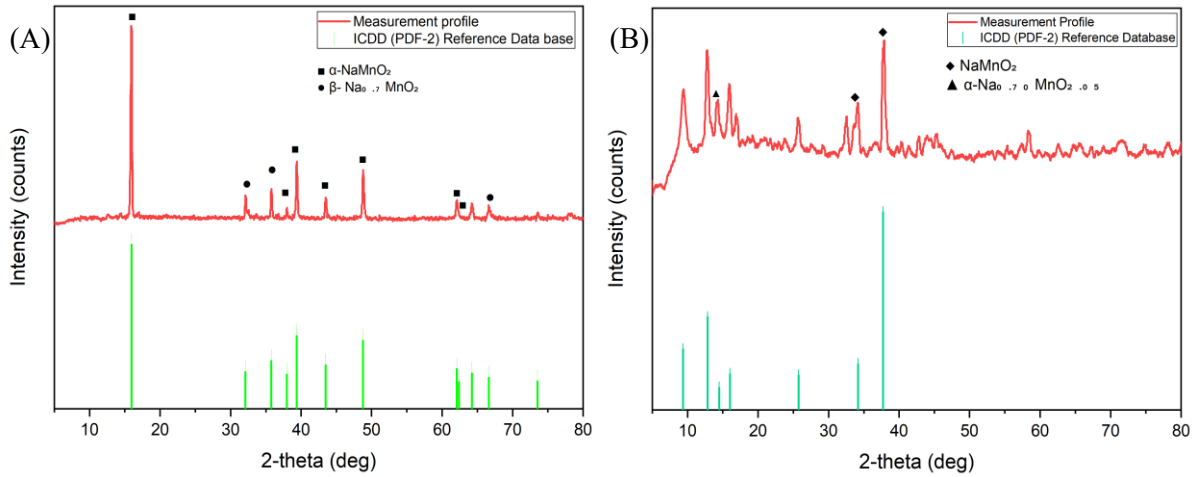

Figure 3: XRD patterns of $NaMnO_2$ synthesized via solid-state reaction using sodium carbonate (Na_2CO_3) with (A) MnO_2 recovered from spent Zn–MnO_2 batteries and (B) analytical-grade MnO_2.

The recovered MnO_2 sample shows formation of multiple sodium manganese oxide phases (β-$Na_{0.70}MnO_2$ and α-$Na_{0.70}MnO_2$), with the most

prominent peaks at 2θ = 15.9° (0,0,2), 32° (2,0, -1), 35.8° (1,1,0), 38° (0,2,2), 39.4° (1,1,2), 43.5° (1,1,3), 48.8° (1,1,4), 62.1° (1,1,6), 62.4° (1,3,0), 66.6° (4,0,-2). The chemical formula is consistently identified as $Na_{0.70}MnO_2$.

The analytical-grade MnO_2 sample demonstrates a phase formation with primarily sodium manganese oxide phases identified at 2θ = 14.5° (0,0,1), 25.8° (2,0,0), 34.18° (2,0,0), and 37.7° (2,0, -2).

The successful formation of sodium manganese oxide phases in both samples confirms the effectiveness of the solid-state synthesis approach, with each precursor offering distinct advantages: recycled material provides higher crystalline intensity.

3.2.2 Evaluation of Recovered MnO_2 from Spent Batteries

The successful synthesis of $NaMnO_2$ using recovered MnO_2 from spent Zn–MnO_2 batteries demonstrates the effectiveness of the extraction procedure and extraction process successfully preserved the essential chemical properties of MnO_2 required for the synthesis reaction. The analysis reveals a significant and unexpected finding: the recovered MnO_2 sample demonstrates enhanced phase purity compared to the analytical-grade material. The recovered sample shows only 17% unidentified phases, while the analytical-grade sample contains 57% unidentified phases.

3.3 Electrochemical Performance Comparison of GO and MEGO Anodes

3.3.1 Discharge Voltage Profiles

The discharge performance of fabricated sodium-ion batteries using GO and MEGO as anode materials was evaluated under constant load conditions with an LED bulb as the external circuit. Figure A and B present the voltage and current profiles during discharge from 3.2V to the cutoff voltage of 1.8V.

The GO-based battery (Figure 4 (A)) demonstrated an initial open-circuit voltage of 3.2V and maintained a more gradual voltage decay throughout the discharge process. In contrast, the MEGO-based battery (Figure 4 (B)) showed a lower initial voltage of 3.0V and exhibited a steeper voltage decline, indicating different electrochemical behaviors between the two anode materials.

3.3.2 Current Density Characteristics

Both anode materials displayed similar initial current densities of approximately 16-17 mA when connected to the LED load. However, significant differences emerged in their current sustainability over time. The GO anode maintained current flow for approximately 180 seconds, while the MEGO anode completely depleted within 90 seconds, representing a 50% reduction in discharge duration.

The current decay profiles reveal distinct electrochemical characteristics: GO exhibited a more controlled and gradual current decrease, suggesting better ionic conductivity and

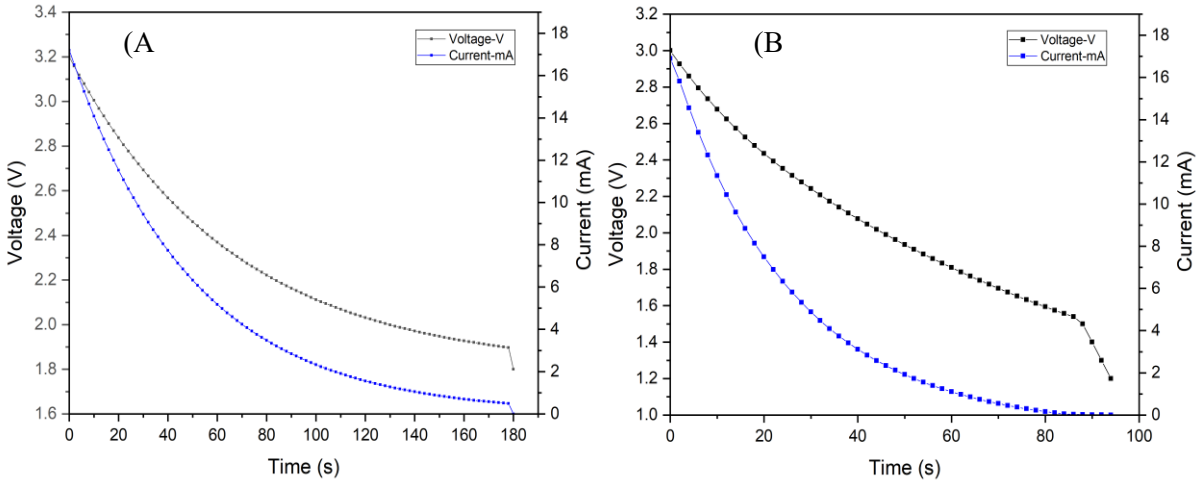

Figure 4 Comparative discharge performance of sodium-ion batteries with different anode materials: (A) GO anode and (B) MEGO anode. Both batteries were discharged under constant LED load.

structural stability during Na^+ intercalation/deintercalation processes. Conversely, MEGO demonstrated rapid current decay, indicating higher internal resistance and possible structural degradation during discharge[8].

3.3.3 Capacity Analysis

Quantitative analysis of the discharge data reveals significant performance differences,

- GO anode: Estimated capacity of ~0.232 mAh
- MEGO anode: Estimated capacity of ~0.107 mAh

The GO anode delivered approximately 2 times higher capacity than MEGO, demonstrating enhanced active material utilization and electrochemical accessibility.

4 Conclusion

This study successfully demonstrates the comparative evaluation of graphite oxide (GO) and microwave-exfoliated graphite oxide (MEGO) as anode materials for sodium-ion batteries. SEM and ImageJ analyses confirmed that microwave treatment effectively increases interlayer spacing and surface roughness; however, this comes with a trade-off in discharge duration compared to GO. These results indicate that GO presents a more

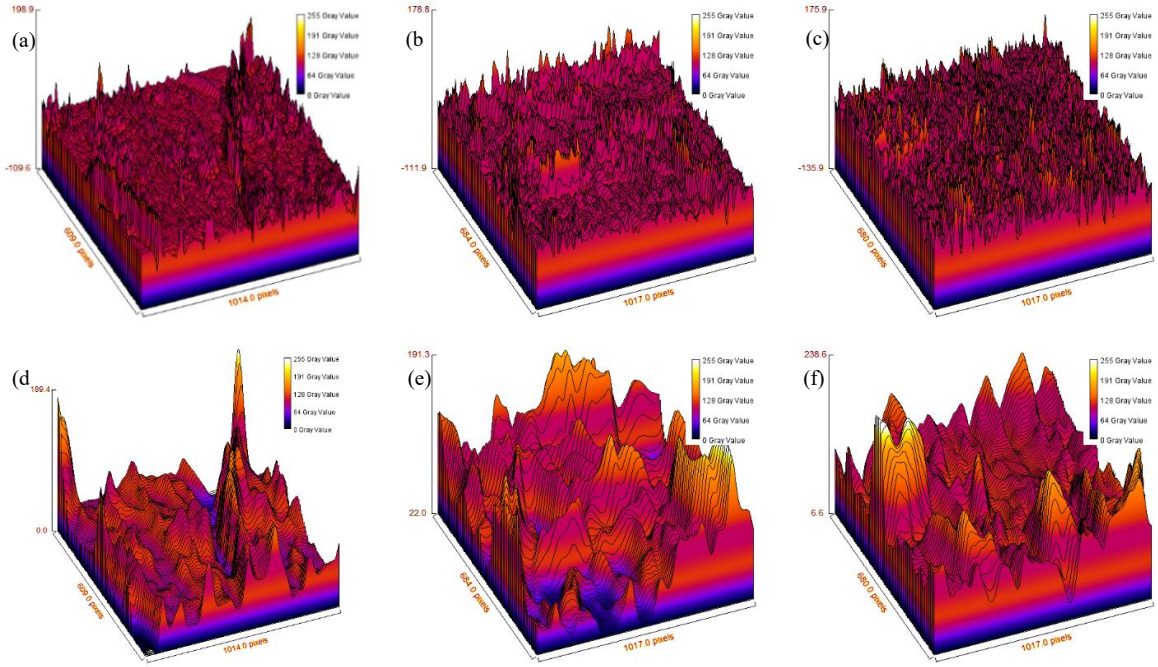

Figure 5 Three-dimensional surface plots representing the roughness and waviness of (a, d) raw graphite, (b, e) graphite oxide (GO), and (c, f) microwave-exfoliated graphite oxide (MEGO, 1-minute exposure), as obtained from SEM images processed in ImageJ using the Waviness/Roughness plugin.

promising anode material for sodium-ion battery applications, offering enhanced capacity retention and more stable discharge characteristics.

The successful synthesis of $NaMnO_2$ cathodes using both recovered and analytical-grade MnO_2 precursors confirms the effectiveness of the solid-state reaction approach. Notably, the enhanced crystalline quality observed in samples prepared from recovered MnO_2 highlights the potential for battery material recycling and supports circular economy practices.

Electrochemical testing of assembled cells revealed that the integration of ethanol-based $NaClO_4$ electrolyte further supports the development of replaceable battery systems.

Overall, this research underscores the importance of material engineering and resource recycling in the development of scalable, sustainable sodium-ion batteries. The findings provide valuable insights into the design of low-cost energy storage devices, particularly in regions with abundant graphite resources, creating new economic opportunities for value-added manufacturing.

Acknowledgement

We express our sincere gratitude to all the academic and non-academic staff of the Department of Earth Resources Engineering for their guidance and support throughout this research. We are especially grateful to Dr. Saranga Diyabalanage for his valuable support during this study.

References

[1] L. Ldnm, R. Ss, M. Il, and R. Lps, "Design and Performance Optimisation of Graphite-Based Batteries for Advanced Energy Storage System."

[2] Yanwu Zhu, Shanthi Murali, Meryl D. Stoller, Aruna Velamakanni, Richard D. Piner, and Rodney S. Ruoff, "Microwave assisted exfoliation and reduction of graphite oxide for ultracapacitors," *Carbon N Y*, vol. 48, no. 7, pp. 2115–2118, Feb. 2010, doi: 10.1016/j.carbon.2010.01.064.

[3] Y. Wen *et al.*, "Expanded graphite as superior anode for sodium-ion batteries," *Nat Commun*, vol. 5, Jun. 2014, doi: 10.1038/ncomms5033.

[4] I. H. Jo *et al.*, "The effect of electrolyte on the electrochemical properties of Na/α-NaMnO2 batteries," *Mater Res Bull*, vol. 58, pp. 74–77, 2014, doi: 10.1016/j.materresbull.2014.02.024.

[5] Z. U. Mahmud, S. Karmakar, A. Haque, and K. C. Ghosh, "A study of fabrication and characterization of NaxMnO2 as a cathode material for sodium-ion battery," *MRS Adv*, vol. 8, no. 15, pp. 828–834, Nov. 2023, doi: 10.1557/s43580-023-00611-4.

[6] J. Guerrero-Contreras and F. Caballero-Briones, "Graphene oxide powders with different oxidation degree, prepared by synthesis variations of the Hummers method," *Mater Chem Phys*, vol. 153, pp. 209–220, Mar. 2015, doi: 10.1016/j.matchemphys.2015.01.005.

[7] M. B. J. G. Freitas, V. C. Pegoretti, and M. K. Pietre, "Recycling manganese from spent Zn-MnO2 primary batteries," *J Power Sources*, vol. 164, no. 2, pp. 947–952, Feb. 2007, doi: 10.1016/j.jpowsour.2006.10.050.

[8] Q. Zhang *et al.*, "A review on energy chemistry of fast-charging anodes," Jun. 21, 2020, *Royal Society of Chemistry*. doi: 10.1039/c9cs00728h.